Analytical Science Advances

WILEY-VCH

Chemistry Europe
European Chemical Societies Publishing

APPLICATION NOTE OPEN ACCESS

In-Tip Nanoreactors for Simultaneous Proteolysis and Enrichment of Phosphorylated Peptides

Ling Yan

College of Science, Eastern Institute of Technology, Ningbo, China

Correspondence: Ling Yan (lyan@eitech.edu.cn)

Received: 26 January 2025 | **Revised:** 3 March 2025 | **Accepted:** 4 March 2025

Keywords: enrichment | matrix-assisted laser desorption/ionization mass spectrometry micropipette tips | nanoporous materials | phosphorylated peptides | proteolysis

ABSTRACT

Protein phosphorylation introduces negative charges on the hydroxyl groups of serine, threonine, and tyrosine residues, reducing the ionization efficiency of phosphorylated peptides. The low abundance of phosphorylated peptides often diminishes their detection using mass spectrometry. To enhance the identification of the low-abundance peptides, an enrichment step was often used, which complicated the high-throughput analysis of phosphorylated proteomes. In this study, we developed a titanium dioxide surface-modified macroporous silicon encapsulated micropipette tips, loaded with trypsin, to integrate rapid enzymatic protein hydrolysis with selective enrichment and extraction of phosphorylated peptides within a microfluidic enzyme reactor. This streamlined approach simplified the protein sample preparation process, combining enzymatic hydrolysis, selective enrichment and separation while maintaining high efficiency. The method enabled comprehensive analysis of complex cancer cell line samples in 1–2 h. Successful detection of phosphorylated peptides from protein mixtures was achieved using matrix-assisted laser desorption/ionization-time-of-flight-mass spectrometry. This application may provide the potential for high-throughput phosphoproteomics and advance the study of protein modifications.

1 | Introduction

Protein phosphorylation, a fundamental post-translational modification (PTM), regulates key biological processes such as cell signalling, proliferation, differentiation, metabolism, and apoptosis [1, 2]. The addition of phosphate groups to serine, threonine, or tyrosine residues alters protein charge and conformation, modulating activity. However, phosphorylated peptides are typically low in abundance and exhibit poor ionization efficiency in mass spectrometry due to their negative charge. Therefore, selective pre-enrichment is essential to enhance detection and distinguish phosphopeptides from their non-phosphorylated counterparts.

Traditional enrichment techniques include immunoaffinity purification with phosphorylation-specific antibodies [3, 4], immobilized metal ion affinity chromatography (IMAC) [5], metal oxide affinity chromatography (MOAC) [6], and their variations with further enhancing selectivity [7–14]. Recent advancements in nanotechnology have introduced novel nanomaterials for phosphorylation research [15]. Notably, porous materials with high surface area and pore volume improve mass transfer and biochemical reactions. Modified porous silicon materials have shown promise in proteomics, particularly for proteolysis and PTM analysis, including phosphorylation [15–18]. Titanium dioxide (TiO_2)-modified macroporous silicon has effectively enriched phosphorylated peptides from complex protein mixtures [19].

The "1-h proteome" concept, introduced in 2014, highlighted the need for faster mass spectrometry workflows [20]. Tip-based

pretreatment methods like StageTips, which simplify protein processing, emerged as promising tools but still rely on overnight proteolysis (12–24 h), limiting efficiency for low-concentration samples [21, 22]. To address this, nanoreactor-encapsulated tips were developed, enabling rapid protein digestion and mass spectrometry analysis of cancer cell proteomes [23]. Further advancements included high-throughput tip reactors for proteomic analysis and drug target identification [24, 25].

This study builds on previous developments by integrating a trypsin-TiO_2-modified macroporous silicon foam (trypsin-TiO-MOSF) nanoreactor into Axygen tips for simultaneous protein digestion and phosphorylated peptide enrichment [19, 23]. Previous studies demonstrated that TiO-MOSF-X outperforms both TiO_2 and IMAC in phosphorylated peptide enrichment, improving signal-to-noise ratio and enhancing the detection of multiple phosphorylated peptides [19]. The large pore volume and surface area of TiO-MOSF material enhance protein adsorption and enable efficient nanoconfined enzymatic reactions. Titanium dioxide species on the surface selectively bind phosphorylated peptides, enriching them within the porous structure while allowing non-specific peptides to flow through. Ammonia elution then collects enriched peptides for mass spectrometry analysis, offering a rapid and efficient solution for PTM research in proteomics.

2 | Materials and Methods

2.1 | Chemical and Materials

The following reagents and materials were used in this study: Poly(ethylene oxide)-poly(propylene oxide)-poly(ethylene oxide) copolymer (P123, MW 5800), methyl orthosilicate (TMOS, 98%), (3-aminopropyl)trimethoxysilane (APTS, 97%), trypsin (≥10000 BAEE units/mg protein), bovine serum albumin (BSA, ≥98%, chromatographic grade), myoglobin (95%–100%), cytochrome C (CYC, ≥95%), beta-casein (β-casein, ≥98%, BioUltra), α-cyano-4-hydroxycinnamic acid (CHCA, ≥98%, TLC), trifluoroacetic acid (TFA, 99%, ReagentPlus) and iodoacetamide (IAA, ≥99%, BioUltra), all obtained from Sigma Aldrich (Shanghai). Dithiothreitol (DTT, 99%) and 2,5-dihydroxybenzoic acid (DHB, >99%) were purchased from Aladdin Reagent (Shanghai). Anhydrous sodium sulfate (≥99%) was sourced from Shanghai Yamato Chemical. Additional reagents included tetrabutyl titanate (≥98%), acetonitrile (ACN, ≥99.8%), ammonium bicarbonate (ABC, 21.0%–22.0% NH_3 content), formic acid (≥88%), ammonia (25%–28%), acetic acid (≥99.5%) and anhydrous sodium acetate (≥99%) from Shanghai Sinopharm Chemical. Phosphoric acid (≥85%) was obtained from Jiangsu Tongsheng Chemical and titanium oxide nanoparticles (P25) from Degussa.

Laboratory consumables included Axygen anti-adsorption and filter micropipette tips (Hangzhou Axygen Biotechnology), a Harris Uni-Core puncher (2.0 mm), and 504 super-purpose adhesives (Beijing Pukairui Biotechnology and Qinfeng Chemical Factory). The enzymatic buffer was prepared with 25 mM ABC (pH ~8), and deionized water (18.4 MΩ·cm) was generated using a Milli-Q system (Millipore, USA). Equipment included a TS-2A/L0107-2A syringe pump (Baoding Lange), B11-3 constant-temperature magnetic stirrer (Shanghai Si Le Instrument), DHG-9031A and DZF-6030 electric and vacuum drying ovens (Shanghai Jinghong Experimental Equipment), a circulating water vacuum pump (Shanghai Shensheng Technology), SX2-4-10 box muffle furnace (Shanghai Yifeng Electric Furnace), FD-27 freeze dryer (Beijing Detianyou Technology) and a Thermomixer Comfort constant temperature mixer (Eppendorf, Germany).

2.2 | Synthesis, Modification, and Characterization of TiO-MOSF

The functionalized tip was loaded with TiO-MOSF, synthesized from unmodified MOSF as previously described [19]. Briefly, MOSF was prepared by stirring P123 and anhydrous sodium sulfate in a 0.2 M HAc-NaAc buffer (pH ~5) at 25°C for 10 h. TMOS was added, and the mixture was stirred at 40°C for 24 h. The product underwent hydrothermal treatment at 100°C for 24 h, followed by calcination at 550°C for 5 h. For TiO-MOSF modification, 0.1 g of MOSF was treated with 50% (v/v) tetrabutyl titanate in ethanol for 30 min, washed with ethanol and water, and calcined at 500°C for 5 h. This process was repeated twice to obtain TiO-MOSF-X (X = 1, 2 and 3, based on the number of treatments).

The materials were characterized using field-emission scanning electron microscopy (FE-SEM), nitrogen adsorption for surface area analysis, Fourier-transform infrared (FT-IR) spectroscopy, Raman spectroscopy, and zeta potential measurements in ABC solution (pH ~7.8).

2.3 | Preparation of Enzyme-immobilized Nanoreactor Encapsulated Micropipette Tips

Trypsin was immobilized on TiO-MOSF-1 to form nanoreactors for protein digestion. TiO-MOSF-1 (0.5 mg) was incubated with trypsin solution in ABC buffer at 25°C for 1 h to facilitate adsorption. Unbound trypsin was removed by washing three times with ABC solution, and the material was resuspended to a concentration of 5 mg/mL.

The nanoreactors were encapsulated in Axygen micropipette tips (T-200-C-L) with a layered design. A 1.3 mm filter was inserted to support the nanoreactor material and 10–100 μL of the 5 mg/mL nanoreactor suspension was added. A second 2.0 mm filter was placed above the material to secure it. The tips were stored at −20°C until use.

2.4 | Protein Digestion and Phosphopeptide Enrichment

The experimental procedure consisted of the following steps (Figure 1): 1) loading large-volume samples through the rear and small-volume samples through the front of the tip; 2) performing infrared light-accelerated proteolysis and peptide enrichment in ~0.5 min for standard protein samples; 3) eluting and collecting phosphorylated peptides; and 4) analyzing the pretreated samples using matrix-assisted laser desorption/ionization mass spectrometry (MALDI-MS).

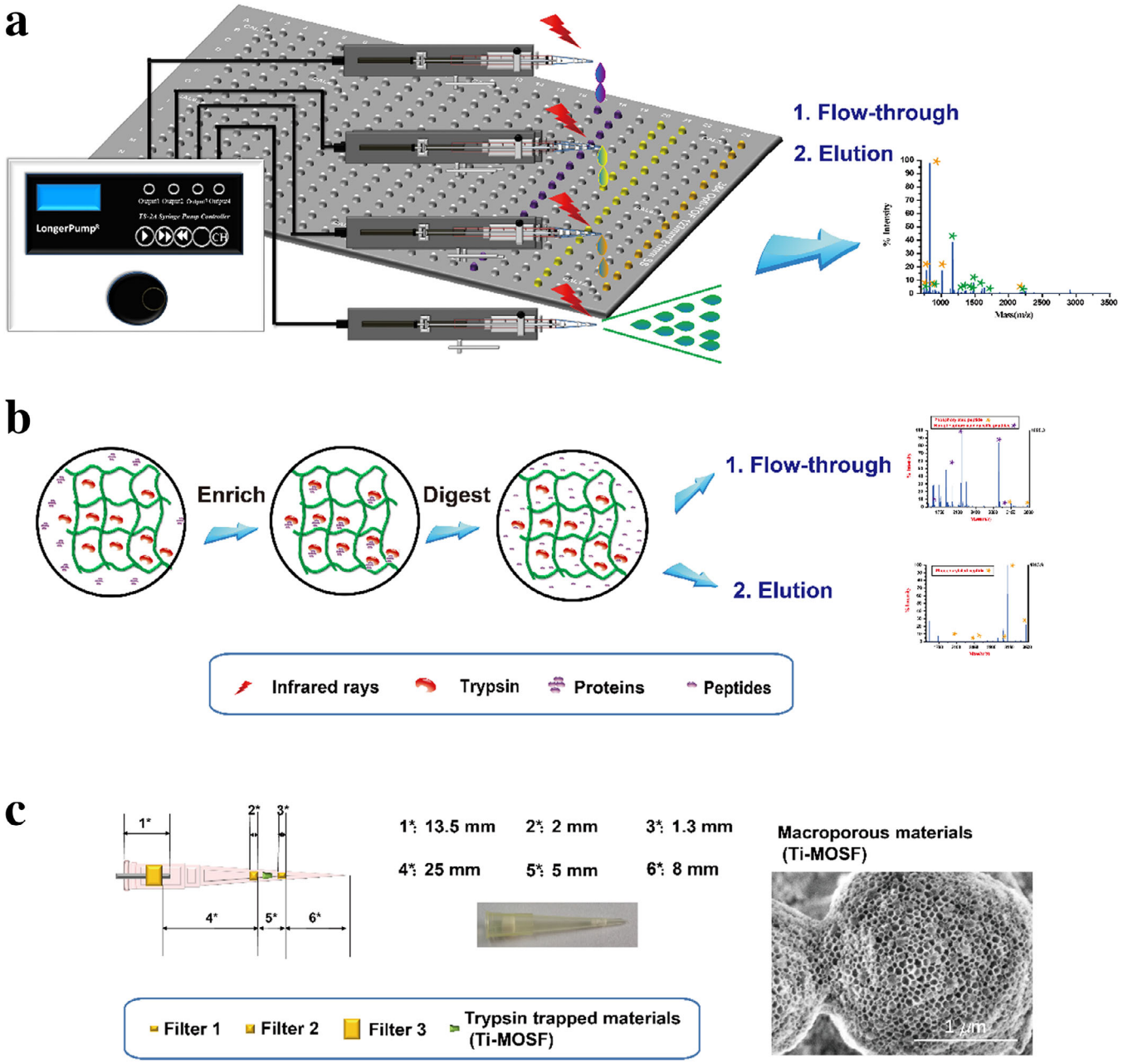

FIGURE 1 | Nanoreactor-loaded micropipette tips and their applications in mass spectrometry (MS) analysis. (a) Experimental flow schematic: peptides were generated at the tip for subsequent matrix-assisted laser desorption/ionization mass spectrometry (MALDI-MS) analysis, with infrared heating maintaining a temperature of ~37°C. (b) Proteolysis and phosphorylation enrichment: trypsin-immobilized nanoreactors facilitate proteolysis and enrichment of phosphorylated peptides, followed by MALDI-MS analysis. (c) Structure and dimensions of the loaded tip, with a field-emission scanning electron microscopy (FE-SEM) image of the macroporous silica.

Functionalized tips were employed for rapid proteolysis and enrichment of phosphorylated peptides. Protein samples (e.g., β-casein) were denatured at 100°C for 5 min and injected into the tip via a syringe pump at controlled flow rates. Proteolysis and peptide enrichment were completed in ~0.5 min. Phosphorylated peptides were eluted with ammonia solution (pH ~10.5) and analyzed by MALDI-MS.

β-casein served as a model substrate for optimizing the digestion process. The tip was washed with ABC solution or DHB solution (20 mg/mL in ACN/H_2O/TFA, 50%/49.9%/0.1% v/v/v), and phosphopeptides were eluted with ammonia solution at a flow rate of 1.67 μL/min. For mixed protein samples (cytochrome C, 100 ng/μL; BSA, 100 ng/μL; and β-casein, 25 ng/μL), a similar procedure was followed, with a flow rate of 6 μL min^{-1}. Eluates were analyzed by mass spectrometry.

As a control, β-casein was digested using a standard in-solution method, incubating denatured β-casein with trypsin (enzyme-to-substrate ratio 1:30, w/w) at 37°C for 12 h with shaking.

TABLE 1 | Matrix-assisted laser desorption/ionization mass spectrometry (MALDI-MS) conditions for analysis of different standard proteins.

	m/z Range	Laser intensity	Bin size (ns)	Matrix	Extraction delay time (ns)	Shots/Sub-spectrum	Total shots
Protein mixture	700–3500	3500	0.5	CHCA	450	100	1000
Beta-casein	1500–3500	4000	0.5	DHB	450	100	1000

2.5 | MALDI-MS Analysis

Proteolysis products and phosphopeptides were spotted onto a MALDI target plate, dried, and overlaid with a DHB matrix solution (20 mg/mL in ACN/H_2O/H_3PO_4, 50%/49%/1% v/v/v). Analysis was conducted using an Applied Biosystem 5800 Proteome Analyzer (Applied Biosystems, California, USA) with an Nd: YAG laser operating at 355 nm, a repetition rate of 400 Hz, and an acceleration voltage of 20 kV. Specific analysis parameters for protein samples are provided in Table 1.

2.6 | Data Analysis

Phosphorylation sites in standard and mixed protein samples were identified using FindMod (http://web.expasy.org/findmod/) with a mass tolerance of ±0.5 Da, allowing up to two missed cleavages, trypsin digestion, and monoisotopic mass values. MALDI-MS data for enzymatic peptides from both standard proteins and protein mixtures were analyzed using the FindPept tool (http://web.expasy.org/findpept/) and MASCOT Peptide Mass Fingerprinting. Peptide identification was performed using the SwissProt Database.

3 | Results and Discussion

3.1 | Characterization of Macroporous Materials

Macroporous materials were characterized by FE-SEM, nitrogen adsorption analysis, Raman spectroscopy, and zeta potential measurements to assess their structural and functional modifications.

FE-SEM images (Figure 2a–d) confirmed that TiO-MOSF-1 maintained a pore diameter of approximately 100 nm, preserving the macroporous foam structure post-modification. Successive modifications increased wall thickness, reduced pore size, and led to crystal formation on the pore surface.

Raman spectroscopy (Figure 3a) identified Si-OH bonds (1000–1100 cm^{-1}) in unmodified MOSF and TiO-MOSF-1, whereas Ti(IV) groups (<800 cm^{-1}) were present in all modified materials. The absence of Si-OH signals in TiO-MOSF-2 and TiO-MOSF-3 confirmed complete surface modification after two coating cycles. Simultaneously, the pronounced Ti(IV) signals (<800 cm^{-1}) in TiO-MOSF-2 and TiO-MOSF-3 indicated the formation of TiO_2 crystals following supersaturation modification. These findings align with nitrogen adsorption results (Table 2), which demonstrated a progressive decline in surface area and pore volume. Compared to unmodified MOSF (464.8 m^2/g, 1.808 cc/g), TiO-MOSF-1 exhibited slightly lower values (366.4 m^2/g, 1.219 cc/g). Further reductions were observed in TiO-MOSF-2 (213.8 m^2/g, 0.543 cc/g) and TiO-MOSF-3 (111.8 m^2/g, 0.437 cc/g), corresponding to 54.0% and 75.9% decreases in surface area and 70.0% and 75.8% reductions in pore volume, respectively. These trends indicate increased wall thickness while maintaining the macroporous framework (Figure 2e–h).

Zeta potential measurements in 25 mM ABC solution (pH ~7.8) (Figure 3b and Table 2) revealed a progressive decrease with successive Ti(IV) modifications. Unmodified MOSF had a zeta potential of −32.5 mV, while TiO-MOSF-1, TiO-MOSF-2, and TiO-MOSF-3 showed zeta potentials of −37.1, −39.5, and −41.4 mV, respectively, aligning with nitrogen adsorption and Raman data.

Excessive TiO_2 crystallization disrupts structural integrity, impeding tryptic digestion and overall performance. In contrast, materials that retain macroporosity, exhibit high surface area, achieve effective Ti(IV) functionalization, and minimize aggregation demonstrate superior efficiency [19]. Among the modified materials, TiO-MOSF-1 provided the best balance of these properties, making it the optimal candidate for enzyme immobilization in nanoreactor applications.

3.2 | Optimization of Trypsin-TiO-MOSF Functionalized Nanoreactor Tips

This study optimized a microfluidic proteolysis platform using TiO-MOSF-1 encapsulated in a pipette tip for efficient protein digestion and phosphorylation peptide enrichment. Unlike traditional methods requiring nanoreactor dispersal, centrifugation, and supernatant collection, the TiO-MOSF-1-based tip offered a streamlined, high-throughput approach. TiO-MOSF-1 immobilized in the tip enabled direct digestion of proteins as samples passed through. Phosphorylated peptides were captured and eluted for mass spectrometry analysis. The modular design allowed flexibility for various proteins.

To minimize nonspecific adsorption, low-adsorption glass injection needles and tips were used. Trypsin, weakly positively charged in ABC buffer (pH ~7.8), was electrostatically immobilized on the negatively charged TiO-MOSF-1. Near-infrared light maintained the reaction at ~37°C, enhancing enzymatic activity. Phosphorylated peptides were captured by TiO-MOSF-1 and eluted with ammonia solution (pH ~10.5) for analysis.

Beta-casein (60 ng/μL) was used to optimize parameters such as the trypsin/TiO-MOSF-1 ratio, material loading, and flow rate (Table 3). A 100 ng/μg trypsin/TiO-MOSF-1 ratio yielded the highest phosphorylated peptide recovery among 25–500 ng/μg, while excessive enzyme loading caused steric hindrance and reduced efficiency. Then, a flow rate of 15 μL/min was selected

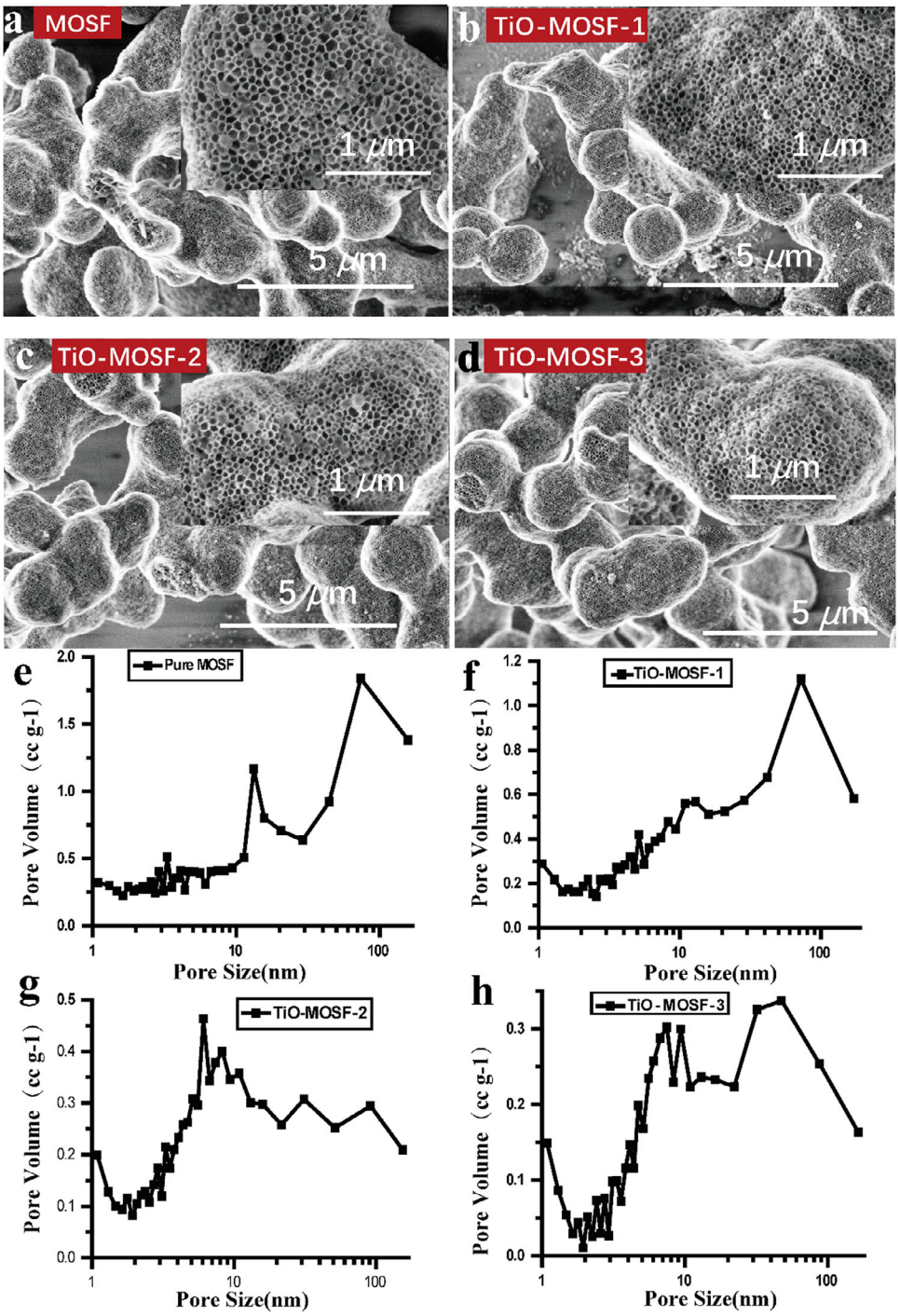

FIGURE 2 | Characterization of nanoreactors. Field-emission scanning electron microscopy (FE-SEM) images of (a) modified macroporous silicon foam (MOSF), (b) TiO_2-modified macroporous silicon foam (TiO-MOSF)-1, (c) TiO-MOSF-2 and (d) TiO-MOSF-3. Pore diameter distributions of (e) MOSF, (f) TiO-MOSF-1, (g) TiO-MOSF-2 and (h) TiO-MOSF-3. Insets in (a)–(d) show partially zoomed FE-SEM images of the materials.

after testing a range of 1.67–20 μL/min, with minor variations in non-phosphorylated peptides across flow rates. Cost-reduction tests maintained the trypsin/TiO-MOSF-1 ratio at 100 ng/μg and flow rate at 15 μL/min, with TiO-MOSF-1 dosages from 50–500 μg. Signal intensity increased up to 250 μg, then plateaued and non-phosphorylated peptide appeared at higher dosages. The criteria for a high recovery rate of phosphorylated peptides are defined as follows: 1) the highest number of phosphorylated peptides; 2) if the number of phosphorylated peptides is equal, the condition with fewer non-phosphorylated peptides is preferred, indicating specificity for phosphorylated peptides; 3) if both phosphorylated and non-phosphorylated peptide counts are equal, the median value of the parameter is selected. The optimized protocol (250 μg TiO-MOSF-1, 100 ng/μg trypsin/TiO-MOSF-1 ratio, 15 μL/min flow rate, ABC buffer for rinsing, ammonia solution (pH ~10.5) for elution at 6.67 μL/min) maximized trypsin-TiO-MOSF-1 tip efficiency for phosphorylated peptide analysis, supporting high-throughput proteomics.

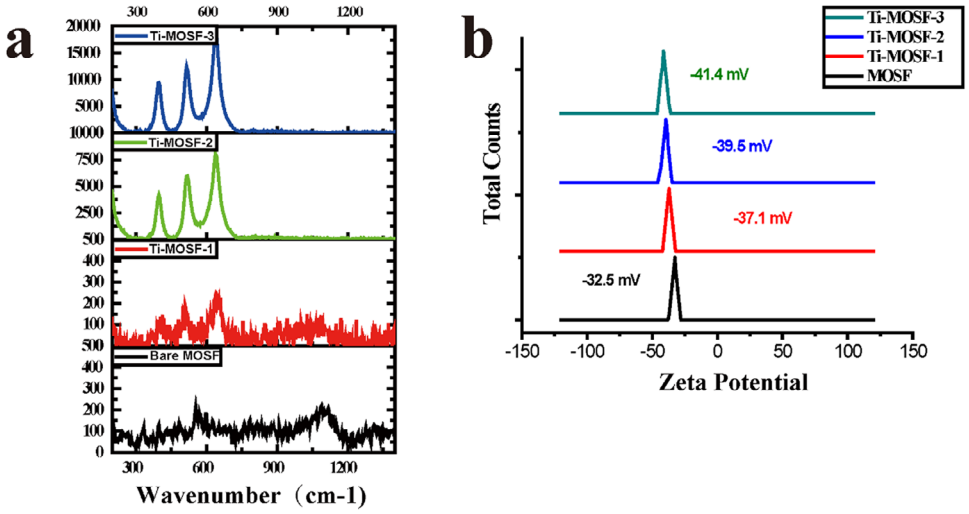

FIGURE 3 | (a) Raman spectra and (b) zeta potential distributions of modified macroporous silicon foam (MOSF), TiO_2-modified macroporous silicon foam (TiO-MOSF)-1, TiO-MOSF-2 and TiO-MOSF-3.

TABLE 2 | Structural properties of the macroporous materials.

Material	Zeta Potential (mV)	Surface area[a] (m^2/g)	Pore volume[b] (cc/g)
MOSF	−32.5	464.8	1.808
TiO-MOSF-1	−37.1	366.4	1.219
TiO-MOSF-2	−39.5	213.8	0.5429
TiO-MOSF-3	−41.4	111.8	0.4373

[a]Barrett-Emmett-Teller (BET) surface area calculated using experimental points at relative pressure of P/P0 = 0.04–0.28.
[b]Calculated by the N2 amount adsorbed at the highest P/P0 (~0.99).

3.3 | Trypsin-TiO-MOSF Functionalized Nanoreactor Tips for Phosphorylated Protein Analysis

Building on prior work developed macroporous silica materials for protein digestion and enrichment, TiO_2-modified MOSF materials were applied to phosphorylated peptide enrichment [19]. In this study, functionalized tips incorporated TiO-MOSF-1 with trypsin in Axygen tips for proteolysis and peptide capture (Figure 1c). Beta-casein (60 μg/mL) was introduced into the trypsin-TiO-MOSF nanoreactor under previously optimized conditions, and digested peptides were analyzed by mass spectrometry. Phosphorylated peptides were captured by the TiO_2-functionalized surface, rinsed with ABC solution, and eluted with ammonia solution (pH ~10.5) for MALDI-MS analysis.

MALDI-MS results of β-casein digests revealed numerous non-phosphorylated peptide peaks and two weak phosphorylated peptide peaks (Figure 4a), indicating effective capture of phosphorylated peptides by the TiO_2-functionalized surface [26–28]. In the ammonia eluate, six phosphorylated peptides were identified without detectable non-phosphorylated peptides (Figure 4b). Therefore, this platform demonstrated efficient, integrated digestion and selective enrichment of phosphorylated peptides, supporting high-throughput proteomic applications. The supporting information provides a detailed discussion of the TiO_2-phosphopeptide interaction mechanisms and the role of the macroporous structure in enhancing this process.

3.4 | Simultaneous Digestion and Enrichment of Protein Mixtures

The performance of the trypsin-TiO-MOSF nanoreactor for complex sample analysis was assessed using a mixture of three standard proteins (100 ng/μL CYC, 100 ng/μL BSA and 25 ng/μL β-casein) under optimized conditions. In this mixture, β-casein, a phosphorylated protein, comprised approximately 10% of the total protein concentration. MALDI-TOF spectrum showed identified results as in Figure 5, while FindPeptides results were summarized in Table S1. Electrostatic interactions during digestion resulted in enhanced proteolysis of the basic protein CYC compared to the acidic protein BSA, with this effect being more pronounced than in the previous trypsin-MOSF nanoreactor immobilized tip. The TiO_2 functional groups specifically bound to phosphorylation sites, facilitating effective proteolysis of low-concentration β-casein and enriching phosphorylated peptides (Figure 5 and Table 4).

Reproducibility tests conducted on five parallel mixed-protein samples revealed robust proteolysis efficiency for CYC, although mixed-protein digestion performance was inferior to single-protein digestion [23]. This discrepancy was attributed to lower protein concentrations, a reduced trypsin-to-protein ratio, and interference from competing proteins, leading to incomplete proteolysis of BSA and β-casein (Table 4). The observed variability primarily stems from the charge and pore size of the TiO-MOSF-1 material in ABC solution, both of which critically influence tryptic digestion efficiency. Zeta potential measurements indicated that TiO-MOSF-1 carries a negative charge in ABC solution, favouring enzymatic hydrolysis of basic proteins like CYC, consistent with prior findings for MOSF [23]. In contrast, acidic proteins such as BSA and β-casein (pI ~5.3) exhibit weaker electrostatic interactions with the material, resulting in diminished digestion efficiency. However, TiO_2 functional groups

TABLE 3 | Matrix-assisted laser desorption/ionization mass spectrometry (MALDI-MS) results for phosphorylated peptides from 60 ng/μL β-casein after digestion, enrichment, and elution of phosphorylated proteins. Elution conditions include variations in trypsin-to-material ratio, sample infusion flow rate, and material amount using trypsin-TiO_2-modified macroporous silicon foam (trypsin-TiO-MOSF) nanoreactor-encapsulated tips.

Optimization parameters	Trypsin/TiO-MOSF-1 (ng/μg)	Flow rate (μL/min)	Amount of TiO-MOSF-1 (μg)	Non-phosphopeptide no.	Phosphopeptide no.
Trypsin-to-material ratio	25	4.45	500	5	1
	50	4.45	500	3	3
	100	**4.45**	**500**	**3**	**4**
	250	4.45	500	3	3
	500	4.45	500	4	3
Flow rate	100	1.67	500	2	5
	100	4.45	500	2	5
	100	6.67	500	2	5
	100	**10**	**500**	**1**	**5**
	100	**20**	**500**	**1**	**5**
TiO-MOSF-1 amount	100	15	50	2	4
	100	15	100	0	4
	100	15	150	0	4
	100	**15**	**250**	**0**	**4**
	100	15	350	1	4
	100	15	500	1	4

Optimization parameters	Trypsin/TiO-MOSF-1 (ng/μg)	Flow rate (μL/min)	Amount of TiO-MOSF-1 (μg)	Non-phosphopeptide no.	Phosphopeptide no.
Trypsin-to-material ratio	25	4.45	500	5	1
	50	4.45	500	3	3
	100	**4.45**	**500**	**3**	**4**
	250	4.45	500	3	3
	500	4.45	500	4	3
Flow rate	100	1.67	500	2	5
	100	4.45	500	2	5
	100	6.67	500	2	5
	100	**10**	**500**	**1**	**5**
	100	**20**	**500**	**1**	**5**
TiO-MOSF-1 amount	100	15	50	2	4
	100	15	100	0	4
	100	15	150	0	4
	100	**15**	**250**	**0**	**4**
	100	15	350	1	4
	100	15	500	1	4

on the TiO-MOSF-1 surface selectively bind phosphorylation sites on β-casein, facilitating efficient enzymatic hydrolysis even at low concentrations. Excessive TiO_2 crystallization on the pore surface reduces pore size, limiting protein accessibility and impairing overall performance. Therefore, to improve reproducibility, two strategies are proposed: 1) Charge modification: Introducing positively charged macroporous materials, such as NH_2-MOSF, could enhance interactions with acidic proteins, as demonstrated in prior studies [23]. 2) Pore size optimization: Refining the TiO_2 modification process to achieve a more uniform distribution of Si-O-Ti bonds and minimize crystallization would preserve the original pore structure, improving protein accessibility and material performance.

Overall, this study highlighted the potential of the functionalized tip for selective proteolysis and high-throughput proteomics, enabling efficient analysis of complex protein samples.

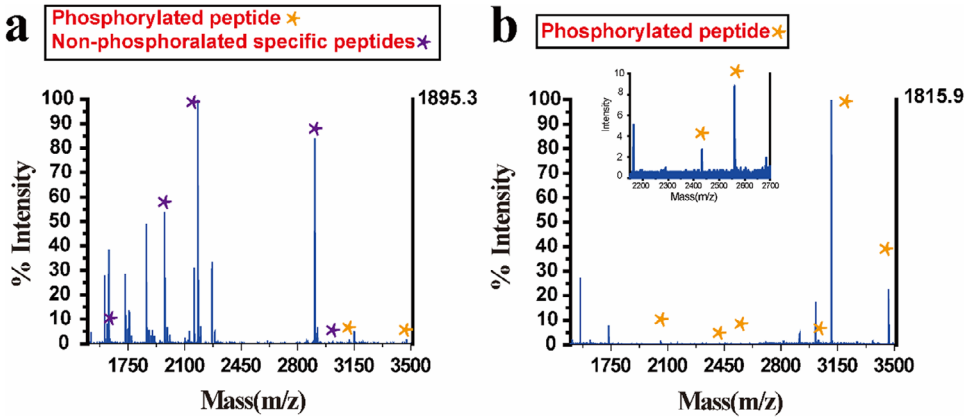

FIGURE 4 | Mass spectra of 60 μg/mL β-casein after digestion with the trypsin-TiO_2-modified macroporous silicon foam (trypsin-TiO-MOSF)-loaded tip. (a) Analysis of the product directly collected from the tip outlet. (b) Peptides eluted from the tip using pH ~10.5 ammonia solution. Specific peptides correspond to tryptic digestion products. TiO-MOSF-1 exhibited an affinity for phosphorylated peptides.

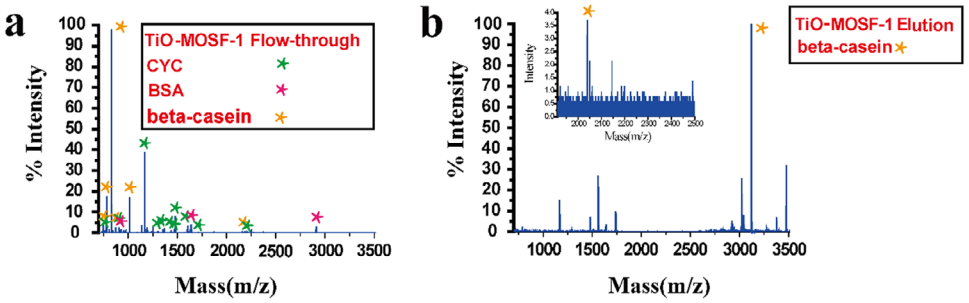

FIGURE 5 | Mass spectra of proteolysis products from a protein mixture of cytochrome C (CYC) (100 ng/μL), bovine serum albumin (BSA) (100 ng/μL), and β-casein (25 ng/μL). (a) Enrichment and digestion catalyzed by the trypsin-TiO_2-modified macroporous silicon foam (trypsin-TiO-MOSF)-loaded tip at a flow rate of 15 μL/min. (b) Peptides eluted with pH ~10.5 ammonia solution following trypsin-TiO-MOSF-loaded tip-catalyzed digestion. This is a representative result from five replicates. Significant peaks corresponding to cytochrome C (CYC), BSA and β-casein are labelled.

TABLE 4 | Reproducibility of the phosphorylated functional tip: MASCOT identification results for peptides digested from a protein mixture of cytochrome C (CYC) (100 μg/mL), bovine serum albumin (BSA) (100 μg/mL) and β-casein (25 μg/mL).

MASCOT results of protein mixtures by using trypsin-TiO-MOSF loaded tips				
Protein name	**Number of times**	**Number of matched peptides**	**MOWSE score**	**Sequence coverage (%)**
CYC	1	18	115	79%
BSA	1	19	36	25%
CYC	2	16	128	76%
CYC	3	16	116	79%
CYC	4	17	117	79%
Beta-casein	4	8	39	31%
CYC	5	13	102	76%
Beta-casein	5	7	40	28%

3.5 | Preliminary Assessment of a TiO_2-functionalized Microreactor for Tryptic Digestion and Enrichment of Phosphorylated Peptides of Bio-samples

This study optimized a TiO_2-functionalized microreactor (trypsin-TiO-MOSF-1) for rapid tryptic digestion and enrichment of phosphorylated peptides from MCF7 cell proteins. The integrated method combined tryptic digestion with TiO_2-based enrichment and was compared to a conventional solution-based approach. Samples were injected into the microreactor at a flow rate of 1.67 μL/min, with a total reaction time of ~6 min. Non-specifically adsorbed peptides were washed with ABC solution, and phosphorylated peptides were eluted with ammonia solution

(pH ~10.5) for nano-liquid chromatography-electrospray ionization-tandem mass spectrometry analysis.

In parallel, the same protein sample was subjected to overnight tryptic digestion followed by TiO_2 nanosphere enrichment. The microreactor method identified 528 proteins and 11 phosphorylated peptides corresponding to five phosphorylated proteins, whereas the conventional method identified 251 proteins and two phosphorylated peptides corresponding to two phosphorylated proteins (Tables S2 and S3).

The lower number of phosphorylated proteins identified may be attributed to the small sample size (1 mg), low phosphorylation levels, and potential losses during sample preparation or one-dimensional separation. Despite these limitations, the microreactor method demonstrated advantages over the traditional approach.

4 | Conclusion

This study first introduced a trypsin-TiO-MOSF-1 nanoreactor-encapsulated tip-based method, designed as a high throughput (6 min for both standard protein and cell lysates) and integrated system for simultaneous proteolysis and enrichment of post-translationally modified proteins. By combining the rapid processing and high efficiency of traditional enzymatic nanoreactors with the precision and simplicity of a microfluidic design, this system enabled streamlined sample preparation through controlled digestion, selective enrichment, and elution via liquid flow adjustments.

Compared to conventional in-solution methods, the proposed platform offered improved efficiency, reduced complexity, and enhanced throughput, making it a cost-effective and user-friendly tool for proteomic and biochemical research. Future optimization of pretreatment for practical bio-samples could focus on two key aspects: (1) enhancing phosphopeptide capture by appropriately reducing sample concentration or adjusting the ratio of trypsin-loaded to unloaded material and (2) minimizing non-specific adsorption of non-phosphorylated peptides by refining elution conditions and employing a combination of rapid and slow washing steps. This approach may provide the potential for high-throughput phosphoproteomics and advance the study of protein modifications.

Acknowledgements

This work is indebted to Prof. Pengyuan Yang and Prof. Baohong Liu from Fudan University for their guidance and support.

Conflicts of Interest

The authors declare no conflict of interest.

Data Availability Statement

The data that support the findings of this study are available from the corresponding author upon reasonable request.

References

1. T. Bilbrough, E. Piemontese, and O. Seitz, "Dissecting the Role of Protein Phosphorylation: A Chemical Biology Toolbox," *Chemical Society Review* 51, no. 13 (2022): 5691–5730.

2. S. Sridharan, A. Hernandez-Armendariz, N. Kurzawa, et al., "Systematic Discovery of Biomolecular Condensate-specific Protein Phosphorylation," *Nature Chemical Biology* 18, no. 10 (2022): 1104–1114.

3. L. Zeneyedpour, C. Stingl, J. M. Kros, et al., "Novel Antibody-peptide Binding Assay Indicates Presence of Immunoglobulins Against EGFR Phospho-site S1166 in High-grade Glioma," *International Journal of Molecular Sciences* 23, no. 9 (2022): 14.

4. F. A. Bhat, K. K. Mangalaparthi, H. S. Ding, et al., "Exploration of Nitrotyrosine-containing Proteins and Peptides by Antibody-based Enrichment Strategies," *Molecular & Cellular Proteomics* 23, no. 3 (2024): 11.

5. R. Z. Tang, Q. Bai, S. J. Ma, et al., "Materials, Workflows and Applications of IMAC for Phosphoproteome Profiling in the Recent Decade: A Review," *Trends in Analytical Chemistry* 158 (2023): 29.

6. B. C. Wang, Z. H. Xie, C. F. Ding, et al., "Recent Advances in Metal Oxide Affinity Chromatography Materials for Phosphoproteomics," *Trends in Analytical Chemistry* 158 (2023): 15.

7. N. Prust, P. C. van Breugel, and S. Lemeer, "Widespread Arginine Phosphorylation in staphylococcus aureus," *Molecular & Cellular Proteomics* 21, no. 5 (2022): 15.

8. L. H. Yi, M. Y. Fu, Y. F. Shao, et al., "Bifunctional Super-hydrophilic Mesoporous Nanocomposite: A Novel Nanoprobe for Investigation of Glycosylation and Phosphorylation in Alzheimer's Disease," *Journal of Chromatography A* 1676 (2022): 11.

9. S. Feng, M. L. Ye, H. J. Zhou, et al., "Immobilized Zirconium Ion Affinity Chromatography for Specific Enrichment of Phosphopeptides in Phosphoproteome Analysis," *Molecular & Cellular Proteomics* 6, no. 9 (2007): 1656–1665.

10. Y. Y. Bian, L. Li, M. M. Dong, et al., "Ultra-deep Tyrosine Phosphoproteomics Enabled by a Phosphotyrosine Superbinder," *Nature Chemical Biology* 12 (2016): 959–966.

11. G. Y. Qing, Q. Lu, X. L. Li, et al., "Hydrogen Bond Based Smart Polymer for Highly Selective and Tunable Capture of Multiply Phosphorylated Peptides," *Nature Communications* 8 (2017): 461.

12. M. M. Li, Y. T. Xiong, and G. Y. Qing, "Innovative Chemical Tools to Address Analytical Challenges of Protein Phosphorylation and Glycosylation," *Accounts of Chemical Research* 56, no. 18 (2023): 2514–2525.

13. Y. Q. Zhao, W. H. Xu, H. J. Zheng, et al., "Light, pH, and Temperature Triple-Responsive Magnetic Composites for Highly Efficient Phosphopeptide Enrichment," *Analytical Chemistry* 95 (2023): 9043–9051.

14. X. J. Zhao, H. J. Qin, M. L. Tang, et al., "Nanopore: Emerging for Detecting Protein Post-translational Modifications," *Trends in Analytical Chemistry* 173 (2024): 117658.

15. X. Y. Lai, J. N. Wang, X. Hu, et al., "The Application of Organic Framework Materials for Peptide Enrichment," *Progress in Biochemistry and Biophysics* 50, no. 3 (2023): 547–560.

16. T. Y. Zhu, Q. Y. Gu, Q. N. Liu, et al., "Nanostructure Stable Hydrophilic Hierarchical Porous Metal-organic Frameworks for Highly Efficient Enrichment of Glycopeptides," *Talanta* 240 (2022): 9.

17. Y. L. Wu, H. L. Chen, Y. J. Chen, et al., "Metal Organic Frameworks as Advanced Extraction Adsorbents for Separation and Analysis in Proteomics and Environmental Research," *Science China-Chemistry* 65, no. 4 (2022): 650–677.

18. S. Swinnen, F. de Azambuja, and T. N. Parac-Vogt, "From Nanozymes to Multi-purpose Nanomaterials: The Potential of Metal-organic Frameworks for Proteomics Applications," *Advanced Healthcare Materials* (2024): e2401547.

19. J. J. Wan, K. Qian, L. Qiao, et al., "TiO_2-Modified Macroporous Silica Foams for Advanced Enrichment of Multi-Phosphorylated Peptides," *Chemistry - A European Journal* 15, no. 11 (2009): 2504–2508.

20. Proteomics. A Proteome in an Hour. *Nature Methods* 10 (2014): 1147.

21. E. Kanao, S. Tanaka, A. Tomioka, et al., "High-recovery Desalting Tip Columns for a Wide Variety of Peptides in Mass Spectrometry-based Proteomics," *Analytical Chemistry* 96, no. 52 (2024): 20390–20397.

22. Z. B. Zhang and N. J. Dovichi, "Seamlessly Integrated Miniaturized Filter-aided Sample Preparation Method to Fractionation Techniques for Fast, Loss-less, and In-depth Proteomics Analysis of 1 μg of Cell Lysates at Low Cost," *Analytical Chemistry* 94, no. 28 (2022): 10135–10141.

23. L. Yan, L. Qiao, J. Ji, et al., "In-tip Nanoreactors for Cancer Cells Proteome Profiling," *Analytica Chimica Acta* 949 (2017): 43–52.

24. Z. L. Ye, P. Sabatier, J. Martin-Gonzalez, et al., "One-Tip Enables Comprehensive Proteome Coverage in Minimal Cells and Single Zygotes," *Nature Communications* 15, no. 1 (2024): 10.

25. Q. Wu, J. N. Zheng, X. T. Sui, et al., "High-throughput Drug Target Discovery Using a Fully Automated Proteomics Sample Preparation Platform," *Chemical Science* 15, no. 8 (2024): 2833–2847.

26. E. T. Tine, J. J. Thomas, N. J. Ole, et al., "Highly Selective Enrichment of Phosphorylated Peptides Using Titanium Dioxide," *Nature Protocols* 1, no. 4 (2006): 1929–1935.

27. T. Garcia-Garcia, T. Douché, Q. G. Gianetto, et al., "In-depth Characterization of the Clostridioides difficile Phosphoproteome to Identify Ser/Thr Kinase Substrates," *Molecular & Cellular Proteomics* 21, no. 11 (2022): 23.

28. Y. J. Ren, J. T. Zhou, M. M. Ali, et al., "Isoform-specific Recognition of Phosphopeptides by Molecular Imprinting Nanoparticles With Double-binding Mode," *Analytica Chimica Acta* 1219 (2022): 9.

Supporting Information

Additional supporting information can be found online in the Supporting Information section.